Available online at www.sciencedirect.com
ScienceDirect
Catalysis Today 133–135 (2008) 394–399
CATALYSIS TODAY
www.elsevier.com/locate/cattod

Tetralin hydrogenation on dealuminated Y zeolite-supported bimetallic Pd-Ir catalysts

A.S. Rocha [a], E.L. Moreno [b], G.P.M. da Silva [a], J.L. Zotin [c], A.C. Faro Jr. [a,*]

[a] *Departamento de Físico-Química, Instituto de Química, Universidade Federal do Rio de Janeiro, Ilha do Fundão, CT, Bl. A, Rio de Janeiro, RJ, CEP: 21949-900, Brazil*
[b] *Fundação Cecierj, rua São Francisco Xavier, 524, 7° andar, Bl. F, Maracanã, RJ, Brazil*
[c] *PETROBRAS/CENPES/HTPE, Ilha do Fundão, Q.7, RJ, 21949-900, Brazil*

Available online 1 February 2008

Abstract

Palladium-iridium catalysts with different proportions between the metals and supported on a dealuminated Y zeolite (SAR ~ 26) had their activity and selectivity measured in tetralin hydrogenation at 523 K and 4 MPa. Characterization of the zeolite support showed that it was free from extra-framework alumina. A palladium-platinum catalyst supported on the same zeolite was also tested for comparison. The metal catalysts were characterized with respect to dispersion by hydrogen and carbon monoxide chemisorption. All of the catalysts displayed moderate deactivation during tetralin hydrogenation and only *cis*- and *trans*-decalin were observed as reaction products. For the same proportion between the metals and the same zeolite support, Pd-Pt and Pd-Ir catalysts had similar activities.

Keywords: Tetralin hydrogenation; Palladium-iridium; Y zeolite

1. Introduction

The combustion properties of diesel fuel for internal combustion engines are relevant for energy conservation and environmental issues. The combustion quality of diesel is measured by its cetane number (CN); the higher the CN, the better the diesel fuel. New environmental restrictions in many countries specify the minimum CN at about 50 [1,2]. Linear and saturated hydrocarbons favor the CN of the diesel, whereas cycloalkanes and especially aromatic compounds are detrimental to this property [3,4]. On the other hand, polyaromatic hydrocarbons present in diesel, on combustion, produce particulate matter in the size range of 0.08–1.0μm. It is respirable and has a significant health impact, with important incidence of allergies in urban areas.

In order to saturate aromatic hydrocarbons, conventional hydrotreating catalysts based on Co–Mo, Ni–Mo or Ni–W sulfides supported on alumina must work at severe operating conditions, which increases the process cost [5]. In this case, noble metal-based catalysts are an interesting alternative, since they have high activity for hydrogenation of aromatic hydrocarbons, and the process can then perform at low temperatures and pressures and high LHSV. However, these catalysts have a low tolerance to sulfur and nitrogen poisoning, therefore a previous deep hydrodesulfurization and hydrodenitrogenation charge pre-treatment is required. This two stage hydrodearomatization (HDA) process has a high operating cost and, consequently, the development of noble metal-based catalysts with tolerance to sulfur and nitrogen has become attractive.

Recently, much interest has arisen in zeolite-supported noble metal catalysts in connection with their application to the hydrogenation of aromatic hydrocarbons contained in petroleum distillates [1,2]. This is because these catalysts have been shown to maintain a useful catalytic activity, even in the presence of relatively high amounts of sulfur compounds (up to several hundred ppm, sulfur basis) [3,6]. As a consequence, economically successful processes have evolved, based on this class of catalysts.

In a previous work, we reported on the sulfur and nitrogen tolerance of Pd-Pt supported on a dealuminated Y zeolite silica–alumina ratio (SAR ~ 25). We found that the pattern of

* Corresponding author.
E-mail address: farojr@iq.ufrj.br (A.C. Faro Jr.).

0920-5861/$ – see front matter
doi:10.1016/j.cattod.2007.12.099

tolerance to nitrogen (as quinoline) of these catalysts, as a function of the proportion between the metals, was similar to that of their tolerance to sulfur (as dibenzothiophene) [6]. However, these catalysts only presented hydrogenation and isomerization activity and no ring-opening products were observed, up to temperatures around 623 K. Decreasing the silica–alumina ratio of the zeolite support (to 17 and 9) caused a decrease in hydrogenation activity, but again no ring-opening could be observed.

Thus, Y zeolite-supported Pd-Pt catalysts do not seem to have ring-opening activity at the temperatures commonly used in noble metal-based HDA processes. On the other hand, recent results show that iridium supported on alumina or zeolites, combined to a catalyst capable of promoting isomerization of five- to six-membered ring, have activity for naphthenic ring-opening reactions [3]. USY-supported bimetallic Pt-Ir catalysts did not present any ring-opening activity, using tetralin as model compound [7], although the bimetallic catalysts had a higher tolerance to sulfur than the monometallic ones. Nevertheless this same bimetallic pair when supported on boehmite presented high activity for opening the indane five-membered ring [8]. Although the Pt-Ir based catalysts present some tolerance to sulfur, the thiotolerance of monometallic iridium catalysts is very low [9].

The questions that remain are: (i) will palladium have the same effect on the thiotolerance of iridium as it has on the thiotolerance of platinum? (ii) will the ring-opening properties of iridium be maintained when combined to palladium? There is much work in the literature with platinum-iridium and palladium-platinum bimetallic catalysts, but not many with palladium-iridium catalysts. In particular, we could not find reference to work with palladium-iridium catalysts for hydrocarbon reactions in the open literature.

In this perspective, the present work is the first part of a study of palladium-iridium catalysts supported on Y zeolite for hydrodearomatization, including the synthesis and characterization of these bimetallic catalysts and their HDA activity under high pressure, using tetralin hydroconversion as a model reaction.

2. Experimental

2.1. Preparation of the catalysts

The catalysts were prepared using as the support a commercial dealuminated HY zeolite, CBV-740, provided by Zeolyst. The zeolite SAR, as measured by infrared spectroscopy, was 25.6, which corresponds to a Y zeolite with unit cell $X_{14}Si_{178}Al_{14}O_{384}{\cdot}nH_2O$, where X is the monovalent charge-compensating cation. The zeolite was submitted to two successive ion exchanges with ammonium chloride solution in order to eliminate any residual sodium, followed by drying and calcination at 673 K, to convert the ammonium-exchanged zeolite to the acid form.

Iridium and palladium were incorporated to obtain catalysts with 5×10^{19} atoms per gram of zeolite, with different proportions between the metals. The nomenclature consists of the nominal palladium atomic percentage with respect to total metals. Bimetallic catalysts were prepared containing 0%, 25%, 50%, 75% and 100% Pd, atomic basis.

First, the palladium was incorporated by ion exchange with appropriate amounts of $Pd(NH_3)_4Cl_2{\cdot}H_2O$, followed by drying and calcination with dry air at 623 K for 4 h. Then, the iridium was incorporated by incipient wetness impregnation with adequate quantities of aqueous solutions of $(NH_4)_3IrCl_6{\cdot}xH_2O$, followed by drying and decomposition under hydrogen flow at 543 K for 2 h and passivation at room temperature. The decomposition of the iridium precursor was carried-out under hydrogen flow in order to avoid metal loss by volatilization of iridium oxides, observed in preliminary experiments.

One Pd-Pt catalyst was prepared using the procedure described previously [6], using the same Y zeolite. Briefly, this procedure involves a simultaneous ion exchange with mixed aqueous solutions of $Pd(NH_3)_4Cl_2{\cdot}H_2O$ and $Pt(NH_3)_4(NO_3)_2$. This sample contained the same metal loading as the Pd-Ir catalysts, 5×10^{19} metal atoms per gram of zeolite, and 75% Pd with respect to total metals, atomic basis.

2.2. Characterization

The sodium content of the zeolite was measured by a flame-photometric method using a Micronal model B262 instrument. The zeolite infrared spectrum in the OH-stretching region was obtained in a Nicolet Magna IR 760 FTIR spectrometer, using a sample cell with CaF_2 windows. Zeolite self-supported wafers with ca. 10 mg cm^{-2} were prepared and pre-treated at 673 K for 4 h under a 10^{-5} torr vacuum before having their FTIR spectra taken at room temperature. The ^{27}Al solid-state NMR spectrum of the zeolite was obtained in a Bruker DRX-300 instrument (7.05 T) using a multinuclear Bruker CP-MAS probe for 4 mm zirconia rotors. A 0.3 μs rf pulse with 0.3 s pulse interval at a spinning speed of 9 kHz were used. The number of transients accumulated was 3000.

The catalysts were characterized by hydrogen and carbon monoxide chemisorption. The chemisorption measurements were performed in an automated volumetric apparatus, ASAP 2010 from Micromeritics, after in-situ reduction with pure hydrogen at 573 K for 2 h followed by evacuation at 583 K for 0.5 h. First, the hydrogen chemisorption was performed followed by evacuation at 583 K for 0.5 h again and the carbon monoxide chemisorption was performed. In both cases, the isotherms were measured at 308 K, in the 0–400 torr pressure range. Two isotherms were obtained for each experiment, with intermediate evacuation for 0.5 h at the analysis temperature to remove weakly adsorbed hydrogen or carbon monoxide. The amount of irreversibly chemisorbed H_2 or CO was obtained from subtraction of the second isotherm (weakly adsorbed H_2 or CO) from the first (total H_2 or CO adsorption).

2.3. Tetralin hydrogenation in a high pressure continuous flow system

The catalytic tests were carried-out in a continuous flow fixed-bed micro-reactor at high pressure, using tetralin (tetrahydronaphthalene) as a model compound. The tests were performed at

4 MPa and 523 K, using a stainless-steel U tube reactor heated in a furnace controlled by a PID controller. The reaction products were analyzed by on-line gas-chromatography (HP 6890 model, with flame ionization detector). The reaction products were identified by GC–MS. Around 0.23 mL min^{-1} of feed (8.8% of tetralin in *n*-hexane) was fed by means of a HPLC pump (Eldex A-60-S) and vaporized in a 300 mL min^{-1} flow of hydrogen (STP). Before the reaction, the catalysts were reduced at 573 K for 2 h in a 200 mL min^{-1} flow of hydrogen.

A rate constant for tetralin conversion after 2 h time-on-stream was calculated (in mol s^{-1} g^{-1}), assuming first order kinetics with respect to tetralin, using the following expression:

$$k = \ln\left[\frac{X}{1-X}\right]\frac{F}{MW} \quad (1)$$

where X is the tetralin conversion, F the reactant flow-rate (3.29×10^{-4} g s^{-1} of tetralin), M the tetralin molar weight (132.21 g mol^{-1}) and W is the catalyst weight (~0.1 g).

Corresponding turnover frequencies (TOF) were calculated from first order rate constants using expression (2) below:

$$\mathrm{TOF} = \frac{k}{N} \quad (2)$$

where N is the amount of metal exposed at the catalyst surface (mol g^{-1}), obtained from CO chemisorption.

3. Results and discussion

3.1. Characterization of the zeolite support

Sodium analysis confirmed that the ion exchange with ammonium successfully removed residual sodium, since the amount of this element in the final zeolite was below the detection limit of the flame-photometric method (0.01 wt.%).

The ^{27}Al NMR spectrum of the zeolite support is presented in Fig. 1A. A peak is observed at around 60 ppm, typical of aluminum in the tetrahedral environment of the zeolite framework. No peaks could be detected at ca. 0 ppm, that would indicate the presence of octahedrally coordinated aluminum ions associated with extra-framework alumina.

Fig. 1B shows the FTIR spectrum of the zeolite in the OH-stretching region. The most intense band occurs at 3740 cm^{-1} and is attributed to silanol groups. Two other bands around 3630 cm^{-1} and 3560 cm^{-1} (HF and LF bands, respectively) are typical of bridged hydroxyls in the supercages and in the sodalite cages of the Y zeolite, respectively [10,11]. The large amount of silanol hydroxyls, evidenced by the intense band at 3740 cm^{-1}, indicates the presence of many defects in the zeolite crystal, which is expected, since this zeolite is highly dealuminated.

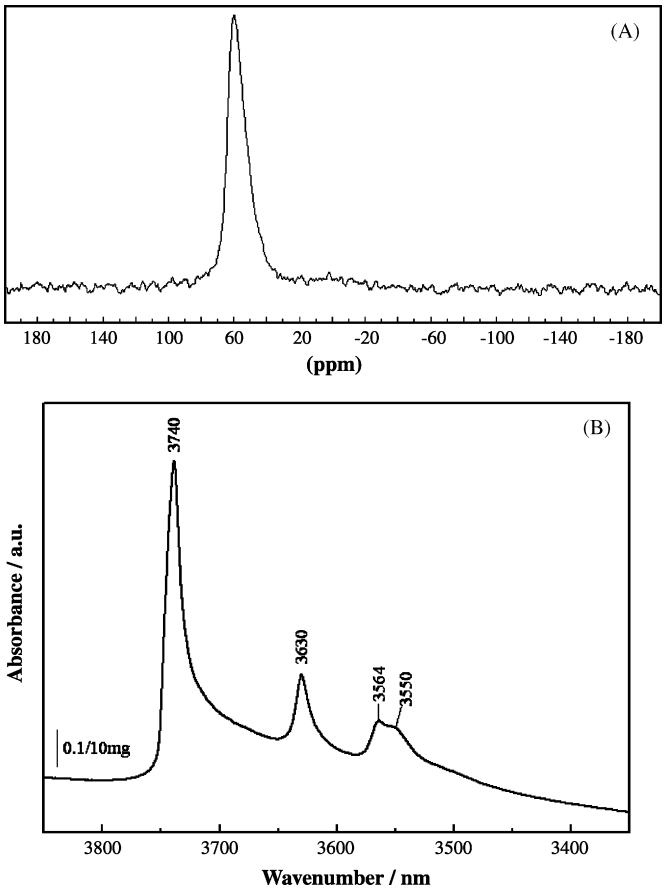

Fig. 1. ^{27}Al NMR spectra (A) and infrared spectra in the OH stretching region (B) of the Y zeolite support.

3.2. Catalysts characterization

Table 1 summarizes the nomenclature and nominal composition of the catalysts. The hydrogen and carbon monoxide chemisorption results obtained by isotherm subtraction are presented Table 2. Dispersion results are also presented, which were calculated assuming a 1:2 H_2 to metal stoichiometry and a 1:1 CO to metal stoichiometry.

The catalysts with the largest iridium contents presented a high capacity for hydrogen chemisorption, consistent with a high dispersion. Although dispersion values above 100% are physically impossible, they can be explained by hydrogen spillover [12] or by multiple adsorptions per site [13].

Kip et al. [13] compared the size of Rh, Ir and Pt particles supported on oxides determined from EXAFS measurements and hydrogen chemisorption. The differences in stoichiometry of adsorption of these metals are large and the H/metal

Table 1
Nominal composition of the catalysts

Catalyst	Ir (wt%)	Pd (wt%)	$(100 \times N_{Pd}{}^{a})/(N_{Pd}{}^{a} + N_{Ir}{}^{b})$
0%Pd-Ir/CBV	1.57	0.00	0
25%Pd-Ir/CBV	1.18	0.22	28
50%Pd-Ir/CBV	0.79	0.44	54
75%Pd-Ir/CBV	0.40	0.66	78
100%Pd-Ir/CBV	0.00	0.88	100

[a] Number of atoms of Pd per gram of catalyst.
[b] Number of atoms of Ir per gram of catalyst.

Table 2
Hydrogen and carbon monoxide chemisorption results

Catalyst	H_2 (cm^3 g)	CO (cm^3 g)	D^a H_2 (%)	D^b CO (%)	H/CO
0%Pd-Ir/CBV	0.921	0.993	101	54.3	1.85
25%Pd-Ir/CBV	0.651	1.28	70.9	69.7	1.02
50%Pd-Ir/CBV	0.486	1.13	52.7	61.2	0.86
75%Pd-Ir/CBV	0.234	0.390	25.2	21.0	1.20
100%Pd-Ir/CBV	0.415	0.641	44.8	34.6	1.29

[a] % Dispersion determined by H_2 chemisorption.
[b] % Dispersion determined by CO chemisorption.

ratio increases in the order Pt < Rh < Ir. The interpretation of the authors is essentially related to multiple adsorption of hydrogen, mainly on the edges and corners of the metallic particles. According to this work, the iridium in an oxidation state higher than 0 is more stable and, as the metal–H bond can be formally described as $metal^+$–H^-, the iridium can accommodate more than one hydride ligand. In the case of iridium particles with about 4 Å, a stoichiometry of 2.7 H/Ir was observed.

Except for catalyst 50%Pd-Ir/CBV, in all cases the H/metals ratio is larger than the CO/metals ratio. This behavior is in agreement with the theory that hydrogen spillover increases the amount of chemisorbed hydrogen beyond the stoichiometric value. However, the very large difference observed with the pure Ir catalyst probably has some influence from multiple adsorptions.

The last column of the table shows the chemisorbed H/CO ratio. If the metals were not interacting in the catalysts, one could expect that H/CO ratio would be a linear combination of the values obtained with the pure metals, according to the surface concentration of each of them. Wong et al. [14] used this fact to estimate the composition of the metal surface in bimetallic catalysts. In the present case, a minimum is observed in this ratio in an intermediate Pd/Ir proportion, indicating that the metals are not only interacting with each other in the bimetallic catalyst, but also that the bimetallic particles have chemisorption properties rather different from those of the monometallic particles.

3.3. Catalytic activity

The possible products of decalin conversion can be grouped as ring-opening, condensation, hydrogenation (*cis*- and *trans*-decalins), dehydrogenation (naphthalene) and isomerization products.

However, for all the catalysts studied, a high selectivity to the hydrogenation products was observed and the added selectivity for all other products was in the order of 2%, for conversions around 40%. In the conditions of the catalytic tests, the catalysts did not present any activity for ring-opening. Also, hydrocracking of the *n*-hexane solvent was not observed.

Fig. 2 shows the activity of the Pd-Ir based bimetallic catalysts for tetralin conversion as a function of time. Considerable catalyst deactivation was observed, especially with the iridium-rich catalysts.

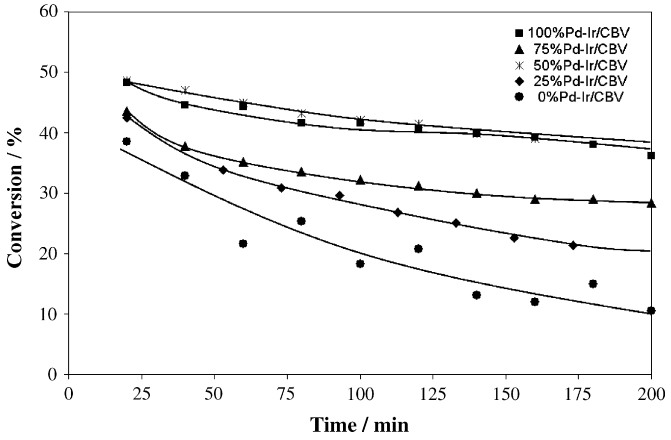

Fig. 2. Conversion of tetralin vs. time-on-stream for all Pd-Ir/CBV catalysts.

The main products observed were the *cis*- and *trans*-decalins. These molecules are structurally similar, but the *trans* isomer is thermodynamically favored. The *cis*/*trans*-decalin ratio varied with time-on-stream, as demonstrated in Fig. 3. For all catalysts this ratio increases with time, at the same time that the catalysts deactivate.

The selectivity for the hydrogenation of double-bonds should be intrinsically *cis*, because at first, the hydrogen attack to the double-bond must occur from the same side of the molecule, i.e., the side that is facing the catalyst surface. According to Weitkamp [15], the formation of the *trans*-decalin in tetralin hydrogenation requires the formation of a Δ1,9-octalin olefinic intermediate, which is formed during tetralin hydrogenation or *cis*-decalin dehydrogenation with the hydrogen in position 10 pointing down to the surface. Therefore, for *trans*-decalin to be formed, it is necessary that this intermediate ''rolls'' on the surface or desorbs and re-adsorbs, so that the hydrogen in position 10 becomes oriented in a direction away from the surface. Then, *cis* hydrogenation of this olefin leads to the *trans*-decalin product. It may then be speculated the behavior observed here with the *cis*/*trans*-decalin ratio is due to the fact that coke deposition in the zeolite cavities impairs the desorption/re-adsorption mechanism responsible for *trans*-decalin formation.

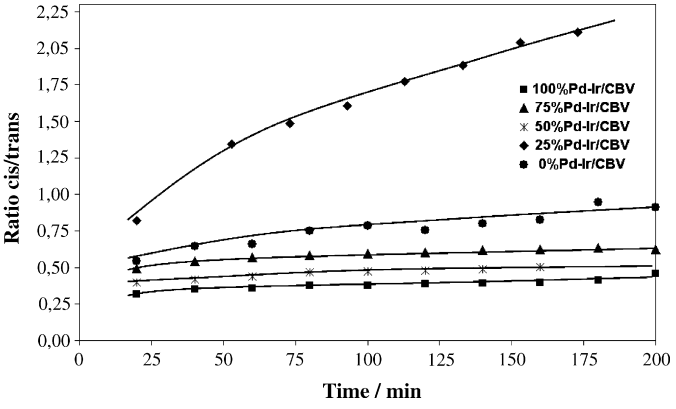

Fig. 3. *Cis*/*trans*-decalin ratio vs. time-on-stream for all Pd-Ir/CBV catalysts.

Table 3
Activity of the Pd-Ir/CBV catalysts

Catalyst	Conversion[a] (%)	$10^6\ k$[b] (mol s^{-1} g^{-1})	TOF from CO chemisorption (s^{-1})
0%Pd-Ir/CBV	21	6.62	0.15
25%Pd-Ir/CBV	25	8.29	0.14
50%Pd-Ir/CBV	42	15.3	0.30
75%Pd-Ir/CBV	31	10.7	0.61
100%Pd-Ir/CBV	41	14.8	0.52

[a] % Measured after 120 min of reaction.
[b] % Calculated using integral conversions assuming a first order kinetics with respect to tetralin.

Larger *cis*/*trans* ratios are observed with the catalysts containing more iridium, i.e., 25%Pd-Ir/CBV and the 0%Pd-Ir/CBV. This behavior can be associated to the strength of the bond between the intermediate that undergoes desorption/re-adsorption and the metal. Iridium is a more hydrogenolysing metal than palladium and it also deactivates more rapidly. This indicates that hydrocarbon intermediates are more strongly bound to its surface. It is expected that a larger strength of adsorption of the Δ1,9-octalin intermediate makes desorption/re-adsorption more difficult [13–15], therefore favoring the *cis* isomer, as observed here.

In terms of conversion and reaction rate (k), a maximum is observed for the catalyst with 50%Pd-Ir/CBV. However, the catalysts differed rather widely with respect to chemisorption capacity. In order to account for this factor, catalytic activities were expressed as turnover frequencies, using the number of active sites of the catalysts determined by carbon monoxide chemisorption. In Table 3 the results for the Pd-Ir catalysts are presented. The values were calculated using the conversion after 120 min and pseudo-first order kinetics. When the TOF is considered, due to the high chemisorption capacity of the iridium-rich catalysts, maximum activity was found with 75%Pd-Ir/CBV.

It should be stressed that we do not assign any fundamental significance to these TOF values, other than simply normalizing the catalytic activities, since the catalyst had not quite reached steady-state activity after 120 min reaction and had considerably deactivated since the beginning of the experiments. However, it is clear from Fig. 2 that no changes in relative order of activity occurred as a consequence of catalyst deactivation. Only carbon monoxide chemisorption data were used in the TOF calculation due to the fact that hydrogen multiple chemisorption on the iridium-rich catalysts and hydrogen spillover may considerably distort the relationship between chemisorption capacity and catalytic activity.

A Pt-Pd bimetallic catalyst containing 75 atom% of Pd and 25 atom% of Pt supported on the same zeolite was tested in the same conditions as the Pd-Ir catalysts. In Fig. 4, activity results are shown as tetralin conversion as a function of time for the two catalysts with 75% of Pd, i.e., 75%Pd-Pt/CBV and 75%Pd-Ir/CBV. It is observed that the two catalysts have very similar activities. The conversion ranges are close and both deactivate with time, however the activity decrease is a little slower in the case of the Pd-Ir catalyst.

Also with the Pd-Pt based catalyst, the decalins are the main reaction products, under our test conditions. As with the Pd-Ir system, the *cis*/*trans*-decalin ratio increases with time-on-stream and were larger in the case of the Pt-Pd system, as shown in Fig. 5. This is consistent with the mechanism discussed previously, since platinum is a less hydrogenolysing metal than iridium and should therefore bind hydrocarbon intermediates more loosely. As explained before, this should facilitate the desorption/re-adsorption of the Δ1,9-octalin intermediate therefore favoring the formation of the *trans* isomer.

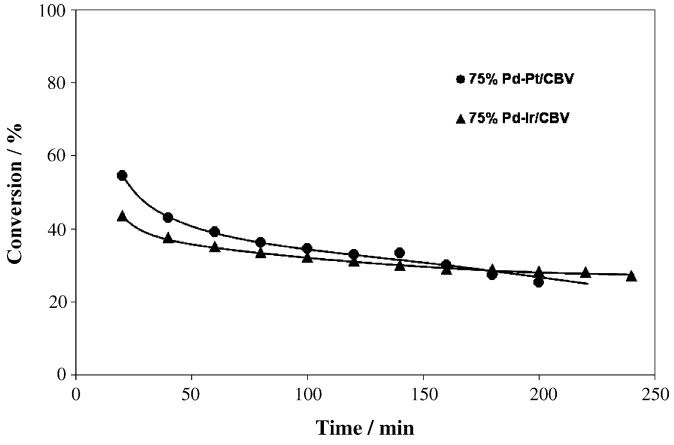

Fig. 4. Tetralin conversion vs. time-on-stream for catalysts with different actives phases, 75%Pd-Ir/CBV and 75%Pd-Pt/CBV.

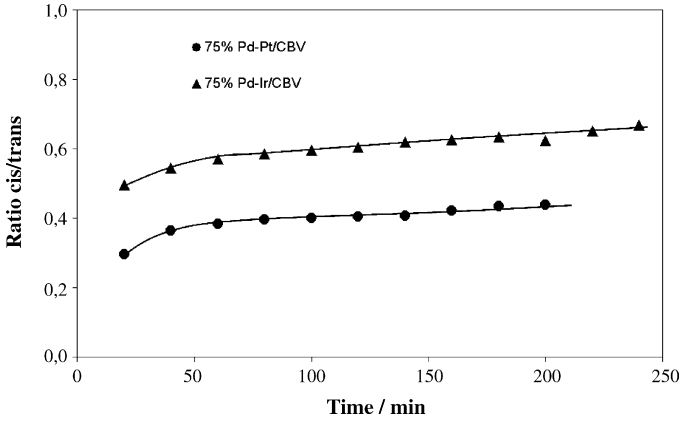

Fig. 5. *Cis*/*trans*-decalin ratio vs. time-on-stream for catalysts with different actives phases, 75%Pd-Ir/CBV and 75%Pd-Pt/CBV.

4. Conclusion

As far as our knowledge goes, there are no previous results in the open literature for hydrogenation of aromatic hydrocarbons on the palladium-iridium bimetallic system.

Results of hydrogen and carbon monoxide chemisorption indicate that, with the preparation method used here, interaction between the metals, i.e., formation of bimetallic particles occurs.

Concerning tetralin hydrogenation, a maximum in intrinsic activity was observed for the catalyst containing 75 mol% of palladium in the metallic phase. This catalyst presented a behavior very similar to that of a palladium-platinum catalyst containing the same molar proportion of palladium and supported on the same zeolite.

The effects of catalyst deactivation, composition of the Pd-Ir catalysts and substitution of Pt for Ir in the bimetallic catalysts on the *cis*/*trans*-decalin ratio is consistent with a previously proposed mechanism [6,16–17], according to which an increase in strength of adsorption of hydrocarbon intermediates on the metal surface renders more difficult the desorption/re-adsorption of the Δ1,9-octalin intermediate responsible for *trans*-decalin formation.

Acknowledgement

We acknowledge financial support by PETROBRAS.

References

[1] H. Topsoe, B.S. Clausen, F.E. Massoth, Catal. Sci. Technol. (1996) 11.
[2] A. Billon, A. Hennico, J.P. Peries, e S. Kressmann, NPRA Meeting, paper AM 91 (1991) 38.
[3] G.B. McVicker, M. Daage, M.S. Touvelle, C.W. Hudson, D.P. Klein, W.C. Baird Jr., B.R. Cook, J.G. Chen, S. Hantzer, D.E.W. Vaughan, E.S. Ellis, O.C. Feeley, J. Catal. 210 (2002) 137.
[4] R.C. Santana, P.T. Do, M. Santikunaporn, W.E. Alvarez, J.D. Taylor, E.L. Sughrue, D.E. Resasco, Fuel 85 (2006) 643.
[5] E. Furimsky, Appl. Catal. A 171 (1998) 177.
[6] C.C.C. Augusto, J.L. Zotin, A.C. Faro Jr., Catal. Lett. 75 (2001) 37.
[7] M.A. Arribas, P. Concepción, A. Martínez, Appl. Catal. A 267 (2004) 111.
[8] U. Nylén, J.F. Delgado, S. Järas, M. Boutonnet, Appl. Catal. A 262 (2004) 189.
[9] R. Frety, P.N. da Silva, M. Guenin, Appl. Catal. 57 (1990) 99.
[10] H. Miessner, H. Kosslick, U. Lohse, B. Parlitz, V.-A. Tuan, J. Phys. Chem. 97 (1993) 9741.
[11] U. Navarro, C.A. Trujillo, A. Oviedo, R. Lobo, J. Catal. 211 (2002) 64.
[12] F.-S. Xiao, B.C. Gates, Stud. Surf. Sci. Catal. 112 (1997) 93.
[13] B.J. Kip, F.B.M. Duivenvoorden, D.C.R. Prins, J. Am. Chem. Soc. 108 (1986) 5633.
[14] T.C. Wong, L.F. Brown, G.L. Haller, J. Chem. Soc. Faraday I 77 (1981) 519.
[15] A.W. Weitkamp, Adv. Catal. 18 (1968) 1.
[16] C.M.M. Guedes, C.C.C. Augusto, J.L. Zotin, A.C. Faro Jr., in Anais do 12° Congresso Brasileiro de Catálise 1 (2003) 376.
[17] A.C. Faro Jr., J.L. Zotin, E.L. Moreno, A.S. Rocha, G.P. de Maria, R. Pinheiro, in Anais do 13 °Congresso Brasileiro de Catálise 1 (2005) 214.